This paper is a preprint of a paper accepted at the 4th International Conference on Vehicle Technology and Intelligent Transport Systems (VEHITS)

Towards Multi-Object Detection and Tracking in Urban Scenario under Uncertainties

Achim Kampker[1a], Mohsen Sefati[1b*†], Arya S. Abdul Rachman[2c*], Kai Kreisköther[1d], and Pascual Campoy[3e]

[1]*Chair of Production Engineering of E-Mobility Components, RWTH Aachen University, Aachen, Germany*

[2]*Delft Center for Systems and Control, Delft University of Technology, Delft, the Netherlands*

[3]*Computer Vision and Aerial Robotics Group, Centre of Automatics and Robotics, Universidad Politécnica de Madrid, Madrid, Spain*

[a]*A.Kampker@pem.rwth-aachen.de,* [b]*M.Sefati@pem.rwth-aachen.de,* [c]*me@AryaSenna.web.id,*
[d]*K.Kreiskoether@pem.rwth-aachen.de,* [e]*Pascual.Campoy@upm.es,* [*]*These authors contributed equally to the paper ,*
[†]*Corresponding author*

Keywords: Multi Object Tracking, Vehicle Perception, 3D LIDAR, Autonomous Driving, Probabilistic Filtering, Heuristics, Rule-based algorithm

Abstract: Urban-oriented autonomous vehicles require a reliable perception technology to tackle the high amount of uncertainties. The recently introduced compact 3D LIDAR sensor offers a surround spatial information that can be exploited to enhance the vehicle perception. We present a real-time integrated framework of multi-target object detection and tracking using 3D LIDAR geared toward urban use. Our approach combines sensor occlusion-aware detection method with computationally efficient heuristics rule-based filtering and adaptive probabilistic tracking to handle uncertainties arising from sensing limitation of 3D LIDAR and complexity of the target object movement. The evaluation results using real-world pre-recorded 3D LIDAR data and comparison with state-of-the-art works shows that our framework is capable of achieving promising tracking performance in the urban situation.

1 INTRODUCTION

The ubiquity of lateral and longitudinal Advanced Driving Assists in contemporary car demonstrates that modern vehicles are able to utilise environmental understanding to gain partial automation in the highway-like situation. It is evident that the case of this technology may not be trivially applicable in an urban situation.

Urban-oriented autonomous vehicles themselves have been extensively researched in body of literature and even tested in (controlled) urban scenario, the latter part is particularly true for the vehicles which have competed in and cleared the DARPA Urban Challenges (Thorpe and Durrant-Whyte, 2009), such as Boss (Urmson et al., 2008), Stanford's Junior(Montemerlo et al., 2008) and MIT's Talos (Leonard et al., 2008). The public demonstration of Project Stadtpilot (Nothdurft et al., 2011) and Project BRAiVE (Grisleri and Fedriga, 2010) further reinforces the feasibility of autonomous cars being ubiquitous in the future road.

There are notable challenges which need to be addressed in urban autonomous driving: first, a large variation of traffic and structures on the vehicle own and adjacent lanes essentially makes the separation between relevant road object from the static terrain even more challenging task. (Leonard et al., 2008).

Second, advancing from typical highway scenario into urban domain also require additional focus on the detection of different classes of traffic object, and especially the addition of Vulnerable Road User (VRU) (Rieken et al., 2015). The need to classify the traffic object and predict its future trajectory (i.e. intent) also arises. Traffic objects also exhibit differing movement pattern which may change within a short timeframe.

Since the vehicle is expected to recognize the intention such objects, the task of vehicle perception is expected to become substantially more complex: not only the vehicle has to detect and derive physical measurement of surrounding objects, but it also has to keep track of multiple dynamic objects in a continuous manner for the reference point of vehicle closed-loop control. Going by this notion, the con-

cept of Multi Object Tracking (MOT) becomes a core essence in vehicle perception.

The recently introduced compact 3D rotating LIDAR scanner (Velodyne, 2007) is especially suitable for this purpose, since it enables far-reaching high fidelity acquisition of surrounding spatial information which is not possible with conventional sensing technologies. LIDAR-based perception tasks geared toward autonomous vehicle is a widely discussed topic. Among others, (Chen et al., 2015) introduces model-based detection for surrounding vehicles (Schreier et al., 2016a) suggest a compact grid-based representation to reliably track uncertain objects also (Himmelsbach and Wuensche, 2012) proposed a top-down bottom-up approach to enhance detection and tracking result while simultaneously doing classification. Notwithstanding, there is a comparably fewer literature which addresses the holistic integration of LIDAR perception tasks aimed toward practical use in the urban situation. (Zhang et al., 2011), (Wojke and Haselich, 2012), and (Choi et al., 2013) notably propose a complete scheme of Multi Object Tracking (MOT). However, these implementation does not specifically target the use-case of urban driving, and limitation of vehicle embedded computer is not necessarily taken into account.

Accordingly, this paper seeks to address the gap by introducing a complete framework of multi-target object detection and tracking using 3D LIDAR which is intended use in the urban scenario; we employ computationally efficient strategies to handle environmental uncertainties. Our approach combines heuristic rule-based logic to prevent obvious improbable detection and tracking hypotheses due to sensor occlusion, and probabilistic adaptive filter to enhance the state estimation and data association process for objects with non-homogenous and crowded nature in the urban situation. Together these approaches strengthen the framework robustness to common uncertainties found in the urban situation and allows more reliable tracking and classification of the static and dynamic property of each object.

First, the point clouds data from the laser sensor is pre-processed by detector component by means of dimensionality reduction: the ground plane is removed, and 2.5-D clusters are formed, then oriented bounding box is fitted into each clustered object to be passed onto tracker component. The tracker employs probabilistic filtering to keep tracks of the detected object in the presence of clutter, sensor occlusion, detection imperfection and manoeuvring targets. Historical information is also used to retain dimensional integrity of the bounding box, and the predicted information from the tracker is passed on to the detector component to augment clustering process in the next time step. Evaluation of tracking performance using established metrics suggest that our strategy shows a favourable result for the purpose of vehicle perception in the urban situation, we also ensure all operations in executed well below sensor sampling rate (10Hz), paving the way to real-time perception in spite of limitation of car embedded computing platform.

2 SYSTEM ARCHITECTURE

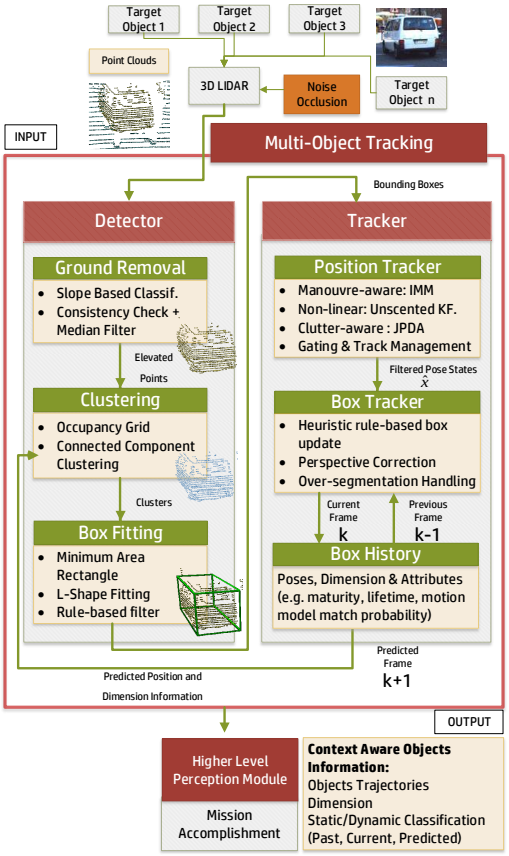

Figure 1: Multi Object Tracking System Architecture

The MOT system consists of two modular part: detector component and tracker component. The component hierarchy and input-output flows can be seen in Figure 1. The input of the system is the raw data from 3D LIDAR scan in point cloud representation of environmental spatial data in Cartesian coordinate, while the output is a list of objects embedded with context-aware attributes, namely the bounding boxes, trajectories and static/dynamic classification. Detector consists of three sub-components which similarly, represent the subtask of detection process: the ground removal, to eliminate object of non-interest and reduce dimensionality of raw data,

clustering, which segment the point clouds into a collection of coherently grouped points (i.e. the object), and bounding box fitting, which embed a uniform object dimension and general direction heading information to each cluster.

The MOT tasks are largely sequential and interrelated, as each component relies on the output of preceding components to perform its task. To exploit this behaviour, the so-called bottom-up top-down approach (Himmelsbach and Wuensche, 2012) is used. The Detector (”top” component) works based on predicted information coming from the Tracker (”bottom” component) to reduce false detection. Since track-by-detection paradigm is used, this approach also augments Tracker component task. The following sections shall elaborate the task and functionality of its sub-components.

3 DETECTOR

3.1 Ground Removal

The raw LIDAR data consists of approximately 3×10^5 points per scan and a large part of the points belong to the ground plane which does not carry meaningful information for tracking purpose. Thus, the first step in measurement pre-processing is the ground removal. In order to address non-planar nature of urban road (e.g. presence of curbs and pedestrian fields), following (Himmelsbach and Wuensche, 2012) the process is done using slope-based channel classification augmented with consistency check and median filtering. The LIDAR measurement with the ground removed is called elevated points and will be used as input for object detection process.

The slope based channel classification determined the ground height by compartmentalizing the LIDAR point clouds and comparing the difference of height (i.e. *slope*) of the successive compartment sequentially starting from a known height reference point. Although this approach is good for smooth terrain, a small, protruding terrain features, such as road bump and grass can still be classified as elevated points. To tackle this, we employ Consistency Check and Median Filtering to flatten the ground plane further and yield better ground estimate.

Consistency Check is done by iterating non-ground cells which are flanked by non-ambiguous ground cells and then comparing the cells' height consistency with the neighbouring cells.Median filtering on the other hand deals with missing ground plane information, as the name implies, the height value of the missing cell is to be replaced with the median value of neighbouring cells. The step-wise results of ground removal can be observed in Figure 2.

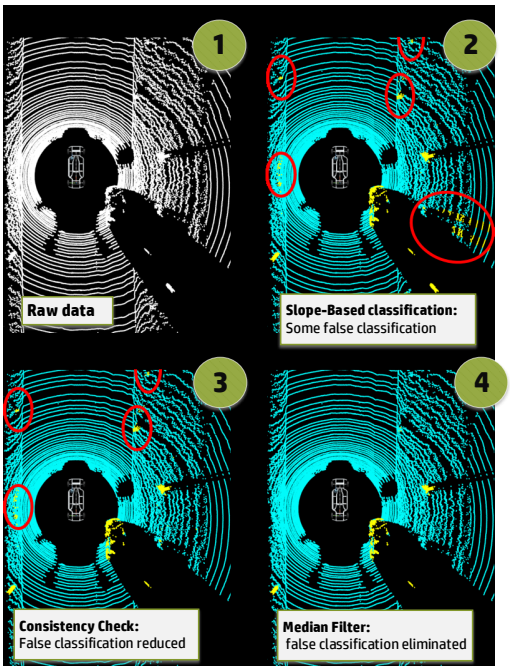

Figure 2: Stepwise ground extraction. Circled is false classification.

3.2 Object Clustering

A tracking of LIDAR individual hits would be computationally infeasible, therefore reduction if dimensionality is required by means of the clustering process. Here, the Connected Component Clusteringis utilised in order to distinguish each possible object in the elevated points. The connected component clustering is originally designed to find connected region of a 2D binary images, however it is also applicable to LIDAR point cloud (Rubio et al., 2013) since in urban situation traffic object does not stack vertically, and thus the top view of the LIDAR measurement can be treated as 2D binary image. Note that the height information is still preserved by referring to the height of the highest Z-axis position point in each cluster relative to the ground.

The XY plane of the elevated points is discretized into grids with $m \times n$ cells. The grid is assigned with 2 initial states, empty (0), occupied (-1) and assigned. Subsequently, a single cell in x, y location is picked as a central cell, and the clusterID counter is incremented by one. Then all adjacent neighbouring cells are checked for occupancy status and labelled with current clusterID. This procedure is repeated for every and each x, y in the $m \times n$ grid, until all non-empty cluster has been assigned an ID.

The clustering process is effective due to discontinuous nature of point cloud. However, its accuracy

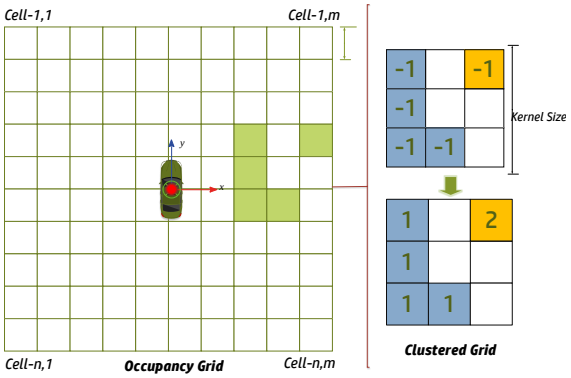

Figure 3: Occupancy Grid and Clustering Result. Left is the discretized grid and right is clustered grid, there are 2 clusters in section of the grid, with clusterID 1 and 2

relies on accurate ground removal in the preceding steps, and a blind spot due to an occluding object in front of sensor viewpoint may lead to over-segmented clusters that otherwise should be part of a single cluster. To handle this issue, the segmentation process is augmented with predicted information from a tracker component which will be discussed in a dedicated section. The LIDAR point cloud ground removal and clustering process final results can be observed in Figure 4.

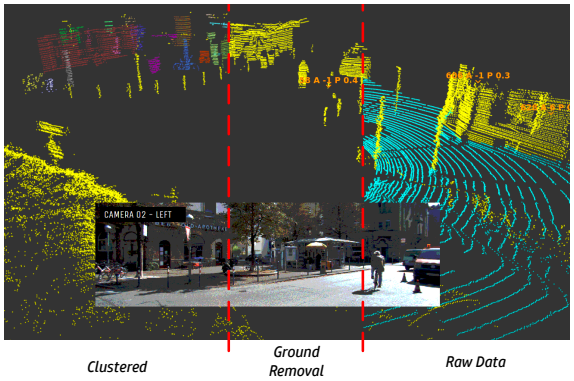

Figure 4: Measurement Pre-Processing: Ground Removal and Clustering

3.3 Bounding Box Fitting

The clustering process produced candidate object to be tracked. To make intuitive semantic information about the object, the bounding box is fitted to have uniform dimensional information and yaw direction. A minimum area rectangle (MAR) (Freeman and Shapira, 1975) is applied to each clustered object which results in a 2D box, and when combined with height information retained in the clustering process, becomes a 3D bounding box (cf. Figure 5).

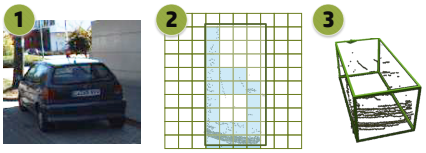

Figure 5: MAR box fitting with embedded height

The MAR approach is not guaranteed to produce correct yaw heading for a non-rectangular cluster (e.g. due to occlusion). To tackle this issue, L-shape fitting (Ye et al., 2016) is used to deduce correct yaw orientation. Two farthest outlier points x_1 and x_2 are selected, and an orthogonal line L_o is projected until a maximum distance to potential corner points is reached, the procedure is illustrated in Figure 6.

The L-shape fitting procedure is done as follows: first, we select two farthest endpoints x_1 and x_2 which lies on the sides of the object facing the LIDAR sensor. A line L_d is then drawn between the two points, then an orthogonal line L_o is projected from L_d toward the available points. The projected L_o with maximum distance and angle close to 90 degrees is then obtained using iteration end-point algorithm. The points connected to the orthogonal line becomes the corner point x_3. Closing a line between x_1, x_2 and x_3 would form an L-shaped polyline. The orientation of the bounding box is then determined by the longest line, as most traffic object (e.g. car and cyclist) is heading in parallel with its longest dimensional side.

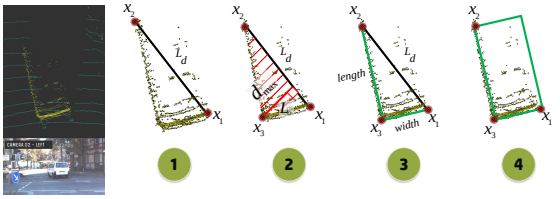

Figure 6: L-shape fitting for better estimate of bounding box orientation

Note that this approach needs a sufficient amount of point to achieve reliable line fitting, so the L-shape fitting is only applicable to car-like object, which correspondingly also suffer from occlusion more than smaller objects such as cyclist and pedestrian, where box representation obtained by MAR approach is deemed sufficient.

4 POSITION TRACKER

Filtering is used to provide optimal estimates of tracked objects trajectory which evolves according to defined motion model regardless of the measurement (i.e. detections result) uncertainty. Here, un-

scented Kalman Filter (UKF) is used in place of Particle Filter and Extended Kalman Filter due to computational constraint consideration (de Feo et al., 1997; György et al., 2014). The targets are assumed to follow stochastic model defined as:

$$\begin{aligned} \mathbf{x}_{k+1} &= f_k(\mathbf{x}_k) + \mathbf{w}_k \\ \mathbf{z}_k &= H(\mathbf{x}_k) + \mathbf{v}_k \end{aligned} \tag{1}$$

with state vector $\mathbf{x}$ and measurement vector $\mathbf{z}$ given as:

$$\begin{aligned} \mathbf{x} &= \begin{bmatrix} x_{pos} & z_{pos} & \psi & v & \dot{\psi} \end{bmatrix}^T \\ \mathbf{z} &= \begin{bmatrix} x_{pos} & z_{pos} \end{bmatrix}^T \end{aligned} \tag{2}$$

and it evolves according to motion model with system function F, and measurement function H. The system is disturbed with zero-mean, white, Gaussian noise sequences $\mathbf{w}$ and $\mathbf{v}$. The centre point of the bounding box (x_{pos}, y_{pos}) and the object yaw rate ψ, velocity v and yaw rate $\dot{\psi}$ are the filtered states at each time step k

The MOT problem can be treated as a single object tracking problem with multiple trackers run in parallel. However, this only work if the objects are moving independently. In urban areas, road users typically move in formation-like motion due to traffic conditions. Although the locations of tracked objects are different; velocity and acceleration may be nearly identical. These measurements with highly correlated motions introduce ambiguities in associating multiple measurements to multiple track tracks. To address this issue, the clutter-aware version of PDAF, the Joint Probabilistic Data Association Filter (JPDAF) (Bar-Shalom et al., 2009) is utilized, it is the extension of PDAF that operates under the assumption that object is tracked under clutter, the situation comes up when different tracks share similar measurements.

Lastly, the state estimation problem relies on the object motion model to predict and update the object states, however in the urban situation, tracked objects do not move in a well-defined pattern. Even if a perfect motion model representing the object trajectories is available, there is no guarantee that the object will follow a specific motion model all the time. The Interactive Multiple Model (IMM) (Genovese, 2001), utilizes multiple models representing different potential target manoeuvres which are run in parallel and continuously evaluated using previous innovation histories. Following (Schreier et al., 2016b) we incorporate 3 different motion model to obtain better estimates of objects with changing dynamics in the urban situation: Linear Velocity Model, Constant Turn-rate and Random Motion Model. The first two models correspond to dynamic objects with predictable motion, while the last model corresponds to noisy detection that usually caused by a static obstacle. The use of IMM also implicitly enable tracker to distinguish between static and dynamic behaviour of tracked objects. Since, dynamic objects move in predictable pattern while noises can be seen to move in a random pattern.

The rationale of the use of JPDAF and UKF is to enable MOT to be run in real-time, alternative statistical DA filter MOT such as Multi-Hypothesis Tracking (MHT) and state filter such as Particle Filter (PF) are shown to be demand more computational load (de Feo et al., 1997; György et al., 2014).

The implementation of IMM-UKF-JPDA consists of four steps: Interaction, Prediction-and-Measurement Validation Step, Data Association-and-Model-Specific Filtering Step, and Mode Probability Update-and-Combination Step. Compared to existing closely related implementation (see (Schreier et al., 2016b)), JPDAF is used instead of the conventional PDAF since we are performing Multi Object Tracking and considering presence of clutter, the association probability β between each track t and measurement j considering all feasible joint association event θ across all measurements Z_k is given by (Bar-Shalom and Li, 1995)

$$\beta_{jt}(l) \equiv= \sum_{\theta:\theta_{jt}\in\theta} P\{\theta_k|Z_k\} \tag{3}$$

and with computed Kalman gain $\mathbf{K}$, and innovation term $\mathbf{z}_k - \hat{\mathbf{z}}_k^-$; the updated system states $\hat{\mathbf{x}}$ becomes .

$$\begin{aligned} \hat{\mathbf{x}}_{k|k} &= \hat{\mathbf{x}}_{k|k-1} + \mathbf{K}_k(\mathbf{v}_k) \\ \text{with } \mathbf{v}_k &= \sum_{m=1}^{N_v} \beta_{m,k}\mathbf{z}_k - \hat{\mathbf{z}}_k^- \end{aligned} \tag{4}$$

4.1 Track Classification

We propose the combined use of velocity and IMM probabilities information (similar to (Schreier et al., 2016a)) as criteria to classify statics and dynamic objects. Generally, an object with zero or negligible relative velocity would be categorized as static. Furthermore, additional checking is done on the IMM probabilities of the three motion models; if the IMM predicts that the probability that the object is moving under Mode-3 (Random Motion) is higher than the other 2 models, then it is statistically likely that an object is a static object.

Naturally, we have to take into account that the estimated velocity is not necessarily smooth, and the IMM probability prediction may take some time steps to converge. To tackle these shortcomings, an average past velocity is used as criteria for static/dynamic classification, additionally a checking if the filter has converged to steady-state value is done before using

the IMM probabilities estimation as the basis of classifying an object as static. The colour-coded classification results can be seen in Figure 7.

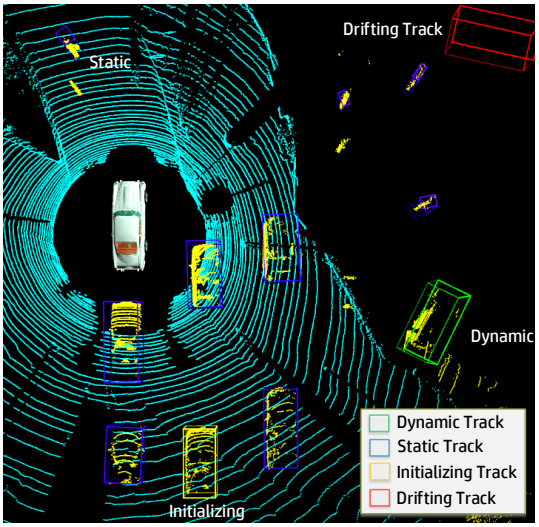

Figure 7: Track Management: colour-coded classification of Track Maturity and Static/Dynamic behaviour. Dynamic track (green) indicates the object is moving, Static track (blue) indicates the object is stopping together with ego-vehicle, Initializing track (yellow) indicates the track not yet matured since the object has just entered the sensor frame, and Drifting track (red) indicates the track is about to be lost due the track entering blind spot area

5 BOUNDING BOX TRACKER

The IMM-UKF-JPDA filter provides estimated poses for point-based object, in order to incorporate dimensional and heading information (i.e. that of bounding box) a logic-based algorithm is implemented which essentially has three major functionalities (1) associate detected box with a track (2) to retain detector best-known output and if later a better detection output is found, update the retained bounding box parameter, (3) perform geometrical correction to compensate occlusion and ego-car perspective change.

The rules are derived from the occlusion characteristic of the LIDAR sensor measurement itself, which is range and viewpoint dependent. The main advantage of the logic-based rule box update the computation load would be negligible. However, since the threshold is based on heuristics, the optimal threshold value can only be obtained through tuning.

5.1 Bounding box association

Since multiple detector box centre points may be associated with the IMM-UKF-JPDAF track, the dimension of the box with the closest Euclidean distance is selected to populate the track dimension information. Gating based on adjustable distance threshold is also done to prevent impossible association. The association criterion is purposely made to be simplistic, since the measurement has actually passed more rigorous gating by the position tracker. In addition, the association of detector bounding box and existing IMM-UKF-JPDA track occurs when the track has met the threshold of maturity and past a predefined threshold of track lifetime. This approach prevents a box belonging to clutter to be associated with a valid track.

5.2 Bounding box dimension and heading

The bounding box fitting approach elaborated assumes *complete* measurement of an object, that is all part of the object is observable. Such measurements themselves can only be obtained when an object falls within a certain range of the sensor and is free from other occlusions. The evolution of the bounding box is illustrated in Figure 8; we see that the dimension of detector bounding box varies according to the position and distance of the tracking target to ego-car. In addition, an occluding object may induce over-segmentation.

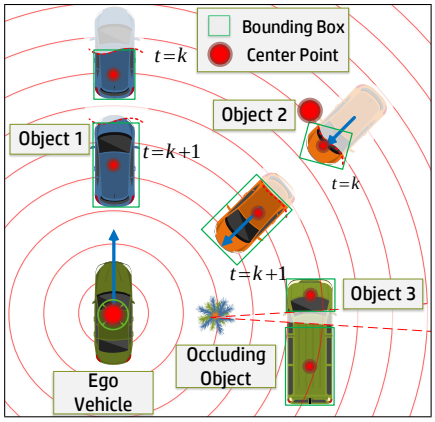

Figure 8: Effect of Occlusion on Bounding Box Fitting.

In this paper, we exploited the following simple, yet precise rules to handle the ever-changing dimension and yaw heading of bounding box: (1) Bounding box area generally should not shrink and length is the parameter that chiefly changes in most case of self-occlusion, (2) Bounding box should never rotate too fast, since traffic objects are generally non-holonomic, and (3) Bounding box should not have sudden movement in opposite direction against the

previous time-steps travel heading (i.e. centre point shifting when box shrink)

We propose the use of the above heuristic rules, to distinguish correct bounding box evolution from noise. In order to realize the rule-based algorithm, the author proposed the use of per-frame history and information from the IMM-UKF-JPDA position tracker. Per-frame history enables the box tracker to store last-known good bounding box at time step $k-n$, where n is adjustable look-back steps parameter. The historical information is to be compared with the newly generated bounding box at time step k. The so-called first last-known bounding box is obtained during bounding box association process described in preceding subsection.

If the newly generated bounding box at k, when compared with that of $k-n$ passed the rule-based filter, then do necessary change: update the dimension, or update the yaw, or do both. Otherwise, retain the last known box if no sane dimension and yaw update is detected. In order to address persistence occlusion, box information from few steps back ($k-n$ step back) is inspected to discern if the box has not been updated for n steps back, which indicates that dimension and/or yaw of the box would need to be updated despite the out of threshold change value. The disadvantage of this threshold-based approach is that it cannot distinguish between small box changes from the noise of detection and real movement of the object. Therefore, the velocity information from the position tracker is used to rule out change of yaw and reduction of dimension for static objects (i.e. zero relative velocity).

5.3 Perspective Correction for self-occlusion

Detected object self-occlusion depends on the perspective of ego-vehicle (cf. centre point shifting in Figure 8). This phenomenon results in inconsistencies in the placement of box centre point. Since the position tracker relies on box centre point for filtering, when self-occlusion occurs, centre point correction needs to be applied to the tracker box using information of last-best known box dimension.

In order to prevent box shifting of an imperfect box caused *not* by self-occlusion. This check is made possible by checking the relative velocity in the longitudinal direction, if the object is moving in the same direction as ego-vehicle, it would be incorrect to shift the box downward and vice versa. Naturally, as even a static object would have a very small velocity due to noise, an adjustable threshold is utilised in the procedure. The shifting results can be observed in Figure 10.

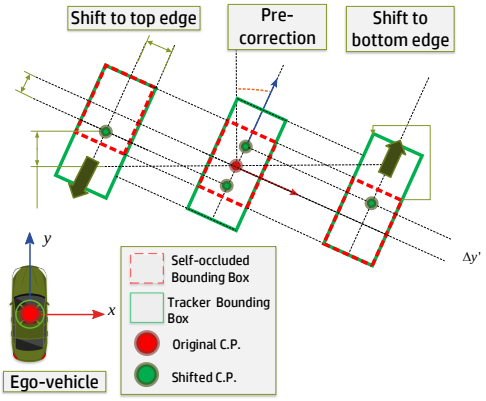

Figure 9: Perspective correction for the bounding box.

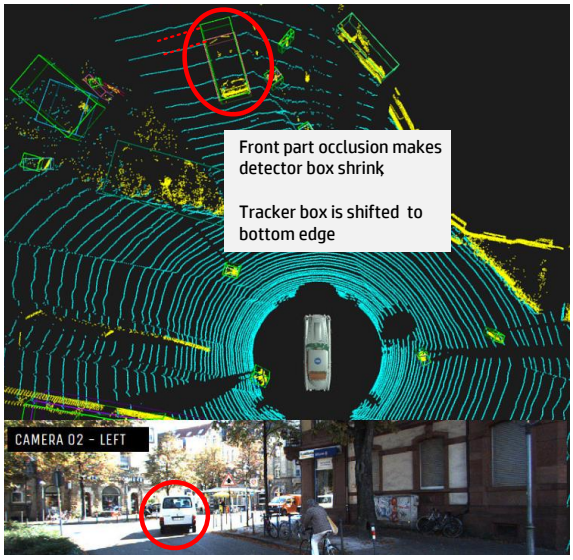

Figure 10: Instance of perspective correction. Self-occlusion of a van located in front of ego-vehicle is shifted downward so that van dimension is retained

5.4 Over-segmentation handling

The segmentation process based Connected Component Clustering relies on a well-defined space between cluster. This space can also inadvertently be created in the case of occlusion caused by another object blocking LIDAR sensor direct line-sight. The occluded area becomes a blind spot and results in over-segmentation. In this case, by utilizing the top-down, bottom-up principle (Himmelsbach and Wuensche, 2012), the tracker component can assist the detector to predict beforehand for such over-segmentation based on the object travel direction and last known good bounding box dimension. (Himmelsbach and Wuen-

Figure 11: Example of over-segmentation handled by box merging

sche, 2012) Notably proposed a similar approach, but instead of dynamically changing the Connected Component Clustering parameter, this paper proposes the use of area percentage threshold to avoid doing repeated steps of clustering.

The over-segmentation handling is made possible by the following procedure: in time step $k-n$ the full dimensioned box already is stored, in addition, the tracker has relative velocity information for all tracked object in each time step. At time step k the detector component then uses the tracker predicted position *prior* to bounding box fitting, if the predicted box encloses or overlaps significantly with the newly generated clusters, then such clusters is to be merged. The procedure, however, may induce under-segmentation, in which two correctly clustered objects located in proximity are incorrectly merged to become a larger cluster. To address this, the newly merged cluster dimension is to be compared against that of the predicted box before the merging is finalized. The exemplary results can be observed in Figure 11 and the procedure can be seen in Figure 12.

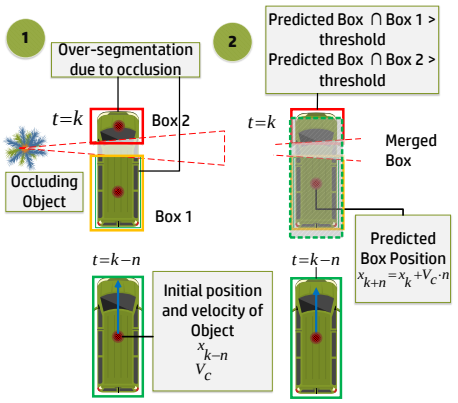

Figure 12: Over-segmentation handling using tracker information

6 EVALUATION

6.1 RAW Data and Ground Truth: KITTI Dataset

In order to verify our MOT system against the real-world situation, it is imperative to use non-synthetic data. For this purpose, the KITTI datasets (Geiger et al., 2013) is used throughout the thesis work. The public dataset provides the recording of LIDAR sensors, among other sensors in the diverse urban driving scenarios in the city of Karlsruhe, Germany. The recording capture real-world traffic situation and range from highways over rural areas to inner-city scenes with high-quality hand-labelled annotation. The sensor used by KITTI team is also Velodyne HDL-64E operating in 10 Hz interval, producing 64 layers of LIDAR data with 0.09-degree angular resolution, and 2 cm distance accuracy. The data stream consists of $\approx$ 1.3 million points/second within 120 m radius of 360 deg horizontal and 26.8 deg vertical field-of-view.

To evaluate the relevant urban situation, KITTI datasets within category "City" is used. The collection of datasets consist of 10 different driving scenarios with the cumulative frame number of 2111 frames and 188 unique traffic objects. The composition of each dataset is represented in Table 1 and Figure 13. Note that the dataset from "City" category contains most relevant VRU class objects compared to other sets and thus more representative to the urban scenario.

Table 1: Evaluation Datasets

Dataset	Frame count	Unique obj.	No. of box
0001	106	11	142
0002	75	2	45
0005	152	14	473
0009	441	82	1413
0013	142	4	101
0017	112	5	84
0018	268	12	196
0048	20	7	81
0051	436	40	381
0057	359	12	471
Sum	**2111**	**189**	**3387**

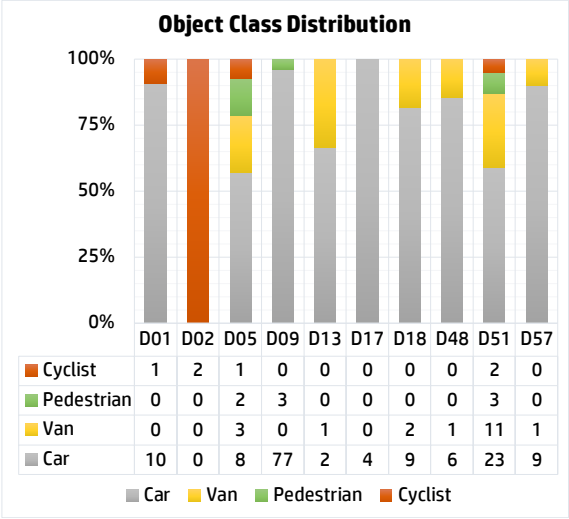

Figure 13: Distribution of object class across all evaluation datasets

6.2 Benchmark Results and Discussion

The tracker performance is to be evaluated using MOT16 benchmark method (Milan et al., 2016) which combines the CLEAR quantitative metric (Bernardin and Stiefelhagen, 2008) augmented with sets of Track Quality Measure (Wu and Nevatia, 2007). We compiled a collection of datasets consisted of 10 different driving scenarios from "City" category with the cumulative frame number of 2111 frames and 188 unique traffic objects. The composition of each dataset is represented in Figure 13. It is important to note the datasets are not a uniform: the driving scenario along with the object composition and movement may vary significantly as the datasets change. This is intentional as tracking methods can be heavily overfitted on one particular dataset and potentially introduced evaluation bias (Milan et al., 2016). Therefore, the individual dataset evaluation result is more of

Table 2: Overall Evaluation Result

(a) CLEAR Metrics

Metrics	Value
MOTA	86.12% ± 6.00
MOTP	91.01% ± 5.03
FP (sum)	65
FN (sum)	406
IDSW (sum)	75
Total Obj. Instances	3387
Total Frame	2111

(b) Tracks quality measures

Metrics	Value
Mostly Tracked	70.64% ± 17.47
Mostly Lost	9.33% ± 8.10
Recall rate	88.92% ± 10.18
Precision rate	98.43% ± 2.73
Fragmentation	211

an accurate indicator to reflect the MOT performance, Nevertheless, it is still useful to view the overall score as shown in Table 1 to aid the reader in grasping the tracker performance.

The Multi Object Tracking Accuracy (MOTA) score reflects that the tracker has a reasonably high degree of accuracy with 86% overall score, the score is lowered chiefly by the number of False Negative (FN), since the number of False Positive (FP) and ID switch (IDSW) are comparatively low. The Multi Object Tracking Precision (MOTP) score is capped at 91% which is expected, since despite perfect tracking, only partial dimensional information can be derived when an object enters the sensor frame from a far distance; so the tracking precision would always be low for first few time frame.

Quality measures-wise, although predictably we see a significant deviation across all datasets, the average results still highlight that the tracker yield higher rate of Mostly Tracked (MT) than Mostly Lost (ML). The recall-rate (i.e. sensitivity) and precision (i.e. positive predictive value) indicate that the tracker hypotheses possess high degree of relevance to the actual object, the lower recall rate is consistent with the number of FN counted in overall. Lastly, the number of Fragmentation is a subset of the FN; here we see the number signals that more than half of FN is caused by track lost that later is able to be successfully resumed, rather than a complete failure of detection across all time frame. To gain more insight into the tracking performance, we inspect the results which belong to the individual dataset. That is since driving scenario varies significantly between datasets.

The MOTP and MOTA scores can be found in Figure 14, the quality measures can be inspected in Figure 15 and the base metrics score can be seen in Table 2.

Some datasets situation will be discussed to give the reader the physical meaning of the results: In Dataset 0005, while 78% of tracks are considered to be MT, we see a relatively large number of ML tracks. Here the ego vehicle is moving in a curved urban road, and this translates into a constantly changing sensor frame of reference. Combination of self-occlusion (cf. Figure 10 for visual depiction) due to sensor angle to the targets and fast (relative) turning rate of target objects increases the uncertainties of the target spatial position (i.e. target are moving rapidly). Therefore, we see a reduced tracking accuracies in this situation, and some tracks suffer from fragmentation. Dataset 0009 represents the most complex driving scenario: it has the largest number of unique objects compared to other datasets, and also comparatively lengthy frame count. In this dataset, the ego car made a 90-degree turn (sudden change of sensor frame) and stopped at a 4-way junction with a known occluding object. The situation can be observed in Figure 11.

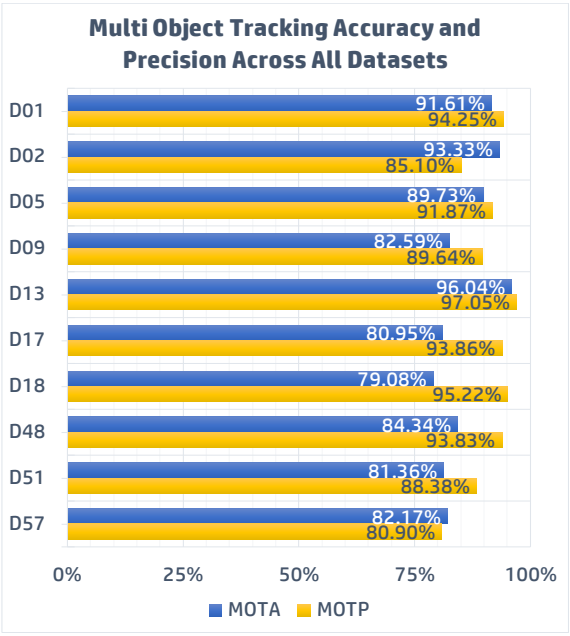

Figure 14: Per dataset MOTA and MOTP scores.

Nevertheless, handling urban situation uncertainties is the main contribution of this thesis: here we see the MOTA score reflects that the use of probabilistic data association and filter enable the tracker to be able to form hypotheses with sufficient accuracy despite clutter and manoeuvring targets. Visible performance degradation is found in select scenario, but since more than 80% of the tracker hypotheses are considered as

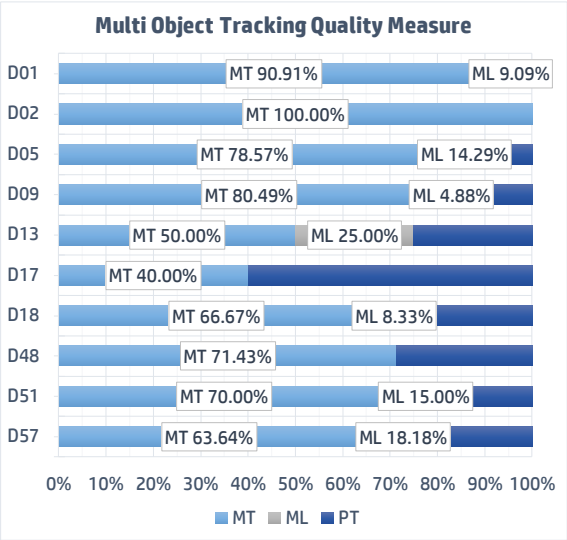

Figure 15: Per-dataset Track Quality Measures. Note that "PT" refers to Partially Tracked, that is the track which is not classified as either MT or ML.

MT, and only 5% are considered as ML, we can see the detector pose an adequate robustness against persistent and self-occlusion of the target objects during the occurrence of sensor frame change, turning cars and other occluding objects. Thus, in Dataset 0009 we see the tracker perform as expected in the presence of environmental uncertainties.

In overall, the benchmarking process yields a better understanding of the tracker performance in a large variation of urban situations and different classes of traffic object. Car, van and pedestrian class object are tracked reliably by an average of above 86% by the MOT system. Quality measures support the scores of the CLEAR metrics, MT tracks outnumber ML tracks by a significant margin in all datasets, including the complex scenario with constant sensor frame change, the presence of persistent occluding object and manoeuvring targets. We see that the accuracy and performance may degrade as number of objects increases and along with the number of self-occlusion and clutter, although the Quality Measures metrics indicate the majority of objects are still covered adequately. Interested reader may refer to the demonstration video in (Abdul Rachman, 2017) to visually inspect the MOT system performance.

7 COMPARISON TO STATE-OF-THE-ART

The use of both established MOT metrics and public dataset are also useful to enable objective comparison to the performance of state-of-art tracker. The utilised metrics, namely the MOTP, MOTA, MT, ML,

Table 3: CLEAR comparison of state-of-art 3D LIDAR trackers

Method	MOTA	MOTP	FN	FP
Proposed Framework	86.12 %	n/a. in m	11.89 %	1.92 %
Tracking Circle (Ye et al., 2016) (averaged)	86.5%	< 0.2 m	3.5%	8.0%
Energy-based (Xiao et al., 2016)	84.2 %	< 0.12 m	5.8 %	2.77 %
BUTD (Xiao et al., 2016)	89.1 %	< 0.16 m	2.6 %	7.6 %
Generative (Kaestner et al., 2012)	77.7 %	< 0.14 m	8.5 %	10.1 %

FN and FP are common measures for tracking performance. Publicly ranked benchmarks (see KITTI Object Tracking Evaluation 2012 (Geiger et al., 2013) and 2017 MOT challenge (Leal-Taixé et al., 2017)) use this metrics, as well as numbers of MOT-related literature(Zheng et al., 2012; Bernardin and Stiefelhagen, 2008; Piao et al., 2016; Wen et al., 2015).

Compared to camera tracking, there is notably fewer LIDAR literature which put significant concern on evaluation using established metrics. Some notable publication which uses both Velodyne and CLEAR as metrics are that of (Ye et al., 2016) which uses geometric-based tracking circle method, (Xiao et al., 2016) which uses point assignment task based on energy function, (Spinello et al., 2011) which uses Bottom-Up Top-Down Detector (BUTD), and (Kaestner et al., 2012) which use Generative Object Detection and Tracking. The comparison results can be seen in Table 3.

These works use different criteria to compute the MOTP. The proposed approach takes account position *and* dimensional integrity of the tracked objects, thus the bounding box overlap ratio is used. Meanwhile, these works consider only the precision of centre point of the detected object, so the MOTP is based on Euclidean distance error instead. In addition, only work of (Ye et al., 2016) deals with a sensor mounted in moving car; the other three use the dataset recorded on ETH Zurich Polyterrasse, which deals with a static frame of reference in university canteen scenery and populated only with pedestrians. (i.e. not remotely close to urban scenario). While results of (Ye et al., 2016) would be the best control comparison to this thesis work, it only uses 2 datasets with unspecified ground truth details.

A general overview indicates our proposed approach has a comparable accuracy ($\pm$ 3% differences) to state-of-art, but accompanied with quite larger percentage of FN (11.89 % vs 2.6% with that of BUTD). In the previous section, it has been found that a large number of FN is contributed by the datasets with complex scenario (mainly Dataset 0017). Nevertheless, if we inspect other datasets individually, the proposed approach FN rate would be on par (2-7%) with other approaches. Therefore, a comparison with standardised datasets is needed to give more insight if the compared state-of-art works exhibit a similar performance degradation in significantly complex urban situation.

8 CONCLUSION

An integrated Multi Object Tracking framework has been introduced in this paper, the framework, in particular, is intended for the use of vehicle perception in the urban situation with the associated uncertainty of 3D LIDAR sensor and tracking targets. The framework encompasses the complete process of multi-object-tracking: it takes raw 3D LIDAR data, and yield context-aware object information that can serve as the basis for the mission accomplishment of higher perception module. The detector is designed to be occlusion and over-segmentation-aware by utilizing consistency check and L-shape fitting in the detector of predicted information exchange with the tracker component. The tracker itself employs probabilistic adaptive filtering based on coupled IMM-UKF-JPDA that allows the tracking of traffic objects characterized by uncertainties in term of motion type and clutter. In addition, the tracker also preserves the dimensional integrity of tracked objects by means of computationally low demanding heuristic rule-based filter and the use box frame history. Finally, evaluation using established MOT16 metric suggest that the tracking performance is favourable in a variety of pre-recorded real-world urban scenarios, and since the framework is designed and found to run in a real-time manner (under 100 ms) we expect that our framework is applicable for real autonomous vehicle deployment.

REFERENCES

Abdul Rachman, A. (2017). Multi-object tracking using 3d lidar in urban situation. *https://aryasenna.net/portfolio/multi-object-tracking-using-3d-lidar-in-urban-situation/*.

Bar-Shalom, Y., Daum, F., and Huang, J. (2009). The probabilistic data association filter. *IEEE Control Syst. Mag.*, 29(6):82–100.

Bar-Shalom, Y. and Li, X. R. (1995). *Multitarget-multisensor Tracking: Principles and Techniques*. Yaakov Bar-Shalom.

Bernardin, K. and Stiefelhagen, R. (2008). Evaluating multiple object tracking performance: The CLEAR MOT metrics. *Eurasip J. Image Video Process.*, 2008.

Chen, T., Dai, B., Liu, D., Fu, H., Song, J., and Wei, C. (2015). Likelihood-Field-Model-Based Vehicle Pose Estimation with Velodyne. *IEEE Conf. Intell. Transp. Syst. Proceedings, ITSC*, 2015-Octob:296–302.

Choi, J., Ulbrich, S., Lichte, B., and Maurer, M. (2013). Multi-Target Tracking using a 3D-Lidar sensor for autonomous vehicles. *IEEE Conf. Intell. Transp. Syst. Proceedings, ITSC*, (Itsc):881–886.

de Feo, M., Graziano, A., Miglioli, R., and Farina, A. (1997). IMMJPDA versus MHT and Kalman filter with NN correlation: performance comparison. *IEE Proc. - Radar, Sonar Navig.*, 144(2):49.

Freeman, H. and Shapira, R. (1975). Determining the minimum-area encasing rectangle for an arbitrary closed curve. *Commun. ACM*, 18(7):409–413.

Geiger, a., Lenz, P., Stiller, C., and Urtasun, R. (2013). Vision meets robotics: The KITTI dataset. *Int. J. Rob. Res.*, 32(11):1231–1237.

Genovese, A. F. (2001). The interacting multiple model algorithm for accurate state estimation of maneuvering targets. *Johns Hopkins APL Tech. Dig. (Applied Phys. Lab.*, 22(4):614–623.

Grisleri, P. and Fedriga, I. (2010). *The BRAiVE autonomous ground vehicle platform*, volume 7. IFAC.

György, K., Kelemen, A., and Dávid, L. (2014). Unscented Kalman Filters and Particle Filter Methods for Nonlinear State Estimation. *Procedia Technol.*, 12:65–74.

Himmelsbach, M. and Wuensche, H. J. (2012). Tracking and classification of arbitrary objects with bottom-up/top-down detection. *IEEE Intell. Veh. Symp. Proc.*, pages 577–582.

Kaestner, R., Maye, J., Pilat, Y., and Siegwart, R. (2012). Generative object detection and tracking in 3D range data. *2012 IEEE Int. Conf. Robot. Autom.*, pages 3075–3081.

Leal-Taixé, L., Milan, A., Reid, I., Roth, S., and Schindler, K. (2017). MOT17 Results.

Leonard, J., How, J., Teller, S., and Berger, e. (2008). A perception-driven autonomous urban vehicle. *J. F. Robot.*, 25(10):727–774.

Milan, A., Leal-Taixe, L., Reid, I., Roth, S., and Schindler, K. (2016). MOT16: A Benchmark for Multi-Object Tracking. pages 1–12.

Montemerlo, M., Becker, J., and Bhat, e. (2008). Junior: The Stanford entry in the Urban Challenge. *J. F. Robot.*, 25(9):569–597.

Nothdurft, T., Hecker, P., Ohl, S., Saust, F., Maurer, M., Reschka, A., and Böhmer, J. R. (2011). Stadtpilot: First fully autonomous test drives in urban traffic. *IEEE Conf. Intell. Transp. Syst. Proceedings, ITSC*, pages 919–924.

Piao, S., Sutjaritvorakul, T., and Berns, K. (2016). Compact Data Association in Multiple Object Tracking: Pedestrian Tracking on Mobile Vehicle as Case Study. *9th IFAC Symp. Intell. Auton. Veh.*, 49(15):175–180.

Rieken, J., Matthaei, R., and Maurer, M. (2015). Toward Perception-Driven Urban Environment Modeling for Automated Road Vehicles. *IEEE Conf. Intell. Transp. Syst. Proceedings, ITSC*, 2015-Octob:731–738.

Rubio, D. O., Lenskiy, A., and Ryu, J. H. (2013). Connected components for a fast and robust 2D lidar data segmentation. *Proc. - Asia Model. Symp. 2013 7th Asia Int. Conf. Math. Model. Comput. Simulation, AMS 2013*, (September 2015):160–165.

Schreier, M., Willert, V., and Adamy, J. (2016a). Compact Representation of Dynamic Driving Environments for ADAS by Parametric Free Space and Dynamic Object Maps. *IEEE Trans. Intell. Transp. Syst.*, 17(2):367–384.

Schreier, M., Willert, V., and Adamy, J. (2016b). Compact Representation of Dynamic Driving Environments for ADAS by Parametric Free Space and Dynamic Object Maps. *IEEE Trans. Intell. Transp. Syst.*, 17(2):367–384.

Spinello, L., Luber, M., and Arras, K. O. (2011). Tracking people in 3D using a bottom-up top-down detector. *Proc. - IEEE Int. Conf. Robot. Autom.*, pages 1304–1310.

Thorpe, C. and Durrant-Whyte, H. (2009). *The DARPA Urban Challenge*, volume 56 of *Springer Tracts in Advanced Robotics*. Springer Berlin Heidelberg, Berlin, Heidelberg.

Urmson, C., Anhalt, J., Bagnell, D., Baker, C., Bittner, R., and Clark, e. (2008). Autonomous driving in urban environments: Boss and the Urban Challenge. *J. F. Robot.*, 25(8):425–466.

Velodyne (2007). Velodyne's HDL-64E: A High Definition Lidar Sensor for 3-D Applications. 2007. *White Pap.*, page 7.

Wen, L., Du, D., Cai, Z., Lei, Z., Chang, M.-C., Qi, H., Lim, J., Yang, M.-H., and Lyu, S. (2015). UA-DETRAC: A New Benchmark and Protocol for Multi-Object Detection and Tracking.

Wojke, N. and Haselich, M. (2012). Moving Vehicle Detection and Tracking in Unstructured Environments. *2012 IEEE Int. Conf. Robot. Autom.*, pages 3082–3087.

Wu, B. and Nevatia, R. (2007). Detection and tracking of multiple, partially occluded humans by Bayesian combination of edgelet based part detectors. *Int. J. Comput. Vis.*, 75(2):247–266.

Xiao, W., Vallet, B., Schindler, K., and Paparoditis, N. (2016). Simultaneous Detection and Tracking of Pedestrian From Panoramic Laser Scanning Data. *ISPRS Ann. Photogramm. Remote Sens. Spat. Inf. Sci.*, III-3(July):295–302.

Ye, Y., Fu, L., and Li, B. (2016). Object Detection and Tracking Using Multi-layer Laser for Autonomous Urban Driving.

Zhang, L., Li, Q., Li, M., Mao, Q., and Nüchter, A. (2011). Multiple Vehicle-like Target Tracking Based on the Velodyne LiDAR. (2005).

Zheng, W., Thangali, A., Sclaroff, S., and Betke, M. (2012). Coupling detection and data association for multiple object tracking. *Comput. Vis. Pattern Recognit. (CVPR), 2012 IEEE Conf.*, pages 1948–1955.